ARTICLES

Self-Assembly of Gold Nanoparticles Prepared with 3,4-Ethylenedioxythiophene as Reductant

Xiaohong Li,[†] Yunchao Li,[†] Yiwei Tan, Chunhe Yang, and Yongfang Li*

Key Laboratory of Organic Solids, Center for Molecular Science, Institute of Chemistry, Chinese Academy of Sciences, Beijing 100080, China

Received: June 11, 2003; In Final Form: February 11, 2004

3,4-Ethylenedioxythiophene (EDOT) was used as the reductant for the first time in the preparation of gold nanoparticles by the reduction of $HAuCl_4$ in THF solution with alkylamine as the stabilizer. During the reduction process of $HAuCl_4$, EDOT was oxidized and oxidatively polymerized. The alkylamine stabilizer and the produced polymer (PEDOT) played a very important role in the subsequent self-assembly of the gold nanoparticles. With trioctylamine as the stabilizer, uniform spherical aggregates (with a diameter of ca. 230 nm) of gold nanoparticles (with a size of ca. 10 nm) were formed. The samples were characterized by TEM, EDS, XRD, XPS, FT-IR, UV−vis, and electrochemical cyclic voltammetry (CV) measurements. The $\pi-\pi$ interaction between the PEDOT coated on the gold nanoparticles was considered to be the driving force for the formation of such aggregates. More interestingly, hollow spherical aggregates composed of smaller gold nanoparticles were observed when higher concentrations of EDOT and trioctylamine were used in the reactive solution. Homogeneous spherical nanoparticles which could self-assemble into an ordered structure were also prepared when dioctylamine was used as the stabilizer. The results indicate that the aggregation states and the morphology of the gold nanoparticles are controllable through changing the concentration of EDOT and trioctylamine or selecting other akylamines as the stabilizer.

1. Introduction

Nanosized Au particles have found many potential applications in technical fields because of their reduced sizes, high surface-to-volume ratio, and relatively high chemical stability in air. For example, colloidal gold particles have been used to label various biological materials, such as antigens, antibodies, enzymes, and so forth, to enable these systems to be observed by transmission or scanning electron microscopy.[1] Small-sized Au particles with diameters less than 5 nm become catalytically active in several chemical reactions when they are supported on certain substrates.[2−4] In particular, uniform monolayer-protected Au nanoparticles can self-assemble into two- or three-dimensional superlattices,[5,6] which are promising for the construction of future nanodevices and nanocircuits.

Several chemical reduction routes of hydrogen tetrachloroaurate(III) for preparing gold colloids have been proposed in the past few decades. The classic citrate reduction method has been extensively utilized to generate aqueous solutions of gold colloids with very narrow size distribution.[7,8] Biphasic syntheses were performed to produce oil-soluble gold colloids (smaller than 5 nm).[9,10] Recently, Au nanoparticles with high colloidal uniformity were prepared in aqueous solution and organic systems by reducing gold salts with *o*-anisidine.[11] Additionally, a series of Au nanoparticles were prepared using ascorbic acid, oxalic acid, or hydrazine as the reducing agents, and it was found that the reactivity and concentration of the reducing agents have a significant effect on the size and dispersity of the metal nanoparticles.[12]

Recently, terthiophene-coated magnetic nanoparticles were produced and self-assembled into uniform spherical aggregates through $\pi-\pi$ interactions.[13] Moreover, a water-soluble terthiophene derivative was used as a reductant for the reduction of $HAuCl_4$ to prepare gold nanoparticles, and terthiophene was oxidation-coupled into sexithiophene in the reaction.[14] Actually, many molecules, such as pyrrole, aniline, thiophene, and so forth, can be oxidized and polymerized into conducting polymers when they are used as reductants to prepare gold nanoparticles. Terthiophene, mentioned above, is an example of the reductants. Therefore, selection of this kind of reductant may create an opportunity in preparing novel aggregation structures composed of Au nanoparticles.

Among conducting polymers, poly(3,4-ethylenedioxythiophene) (PEDOT), which possesses remarkable transparent-conducting and electrochromic properties, has been employed in the ITO electrode modification of polymer light-emitting diodes,[15] the preparation of antistatic, transparent coating,[16,17] and the metallization of insulating devices.[18] The oxidation potential of EDOT is close to that of terthiophene, which makes it possible for it to be used as the reductant in the preparation of Au nanoparticles. In this paper, we used EDOT as the reductant to reduce $HAuCl_4$ in THF solution, and the gold nanoparticles were obtained successfully with alkylamine as the stabilizer. Interestingly, the as-prepared gold nanoparticles self-assembled into uniform spherical aggregates or hollow spherical aggregates

* Corresponding author. E-mail: liyf@iccas.ac.cn.
[†] Also at the Graduate School, Chinese Academy of Sciences, Beijing, China.

10.1021/jp0356618 CCC: $27.50
Published on Web 04/03/2004

when trioctylamine was used as the stabilizer. Moreover, different nanostructures were also obtained by changing the concentrations of EDOT and trioctylamine or selecting different kinds of alkylamine such as dioctylamine as the stabilizer.

2. Experimental Section

2.1. Materials. Hydrogen tetrachloroaurate(III) ($HAuCl_4$), trioctylamine, dioctylamine, and THF were purchased from Aldrich and used without further purification. 3,4-Ethylenedioxythiophene (EDOT) was obtained from Bayer Company (Germany) and was purified by distillation under reduced pressure before use. The water used was purified by distillation of deionized water. All the solvents used in this work were purged with dry nitrogen for 30 min before use.

2.2. Synthesis of Gold Colloids. *2.2.1. Preparation of Gold Nanoparticles Using Trioctylamine as the Stabilizer.* The synthesis of Au nanoparticles was carried out by the chemical reduction of $HAuCl_4$ in THF solution with EDOT as the reductant and trioctylamine as the stabilizer. The following reduction methods with different concentrations of EDOT and trioctylamine were employed.

Method I. A 17 mL THF solution containing 10 μL (0.1 mmol) of EDOT was heated to 120 °C and kept at that temperature for 5 min under refluxing conditions and was stirred to ensure full mixing of the reaction reagents. To the heated mixture, 3 mL of THF solution containing 0.8 mL of $HAuCl_4$ (50 mM) aqueous solution and 50 μL of (0.1 mmol) trioctylamine were added quickly. Then the reaction mixture was continuously heated at 120 °C for 8 h under vigorous stirring. A red-yellow Au colloidal solution was obtained at the end of the reaction.

Method II. The method is similar to method I except that 30 μL of EDOT was added and refluxing conditions were kept for 5 h.

Method III. The method is similar to method II except that 40 μL of EDOT was added in the reaction solution.

Method IV. The method is similar to method III except that 200 μL of trioctylamine was added as the stabilizer in the reaction system.

Pale green-yellow Au colloidal solutions were obtained at the end of the reactions with methods II−IV.

2.2.2. Preparation of Gold Nanoparticles Using Dioctylamine as the Stabilizer. Method V. The method is similar to that of method II except that 47.2 mg (0.196 mmol) of dioctylamine instead of trioctylamine was used as the stabilizer. A green-yellow Au colloidal solution was obtained at the end of the reaction

2.3. Characterization. The formation process of the Au colloidal solution was monitored by UV−vis absorption spectroscopy with a HITACHI U-3010 UV−vis scanning spectrophotometer. The Au colloids were characterized by transmission electron microscopy (TEM), energy-dispersive X-ray spectroscopic (EDS) analysis, selected area electron diffraction (SAED), and high-resolution TEM (HRTEM) images. TEM was performed on a JEOL-JEM-100CX II transmission electron microscope operated at 100 kV accelerating voltage. The HRTEM images were acquired with a JEOL-JEM 2010F transmission electron microscope operated at 200 kV. The samples for TEM measurements were prepared by placing a drop of the freshly prepared colloidal solution onto a carbon-coated 300-mesh copper grid and allowing it to dry in air naturally. EDS analysis using a 0.7 nm diameter electron probe was employed to determine directly the chemical identities of the constituent particles. The measurements were conducted by illuminating

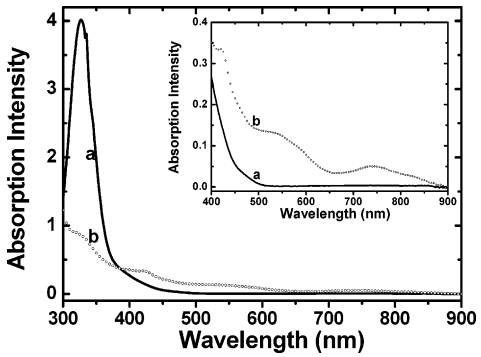

Figure 1. UV−vis absorption spectra of the Au colloid prepared by method I: (a) before refluxing; (b) after refluxing for 8 h.

electron beams on a whole particle. The X-ray diffraction (XRD) measurement was carried out in the reflection mode on a Rigaku D/max-2400 diffractometer operated at a voltage of 40 kV and a current of 120 mA with Cu Kα radiation. X-ray photoelectron spectroscopy (XPS) data were obtained on a VG-Scientific ESCA Lab 220i-XL spectrometer equipped with a hemisphere analyzer, a multichannel detector, a toroidal monochromator, and an Al Kα X-ray source at 1486.6 eV. Peak positions were internally referenced to the C1s peak at 284.6 eV. The sample for the XPS measurement was prepared by the following process: The Au nanoparticles were precipitated by rotary-evaporating the colloidal solution; then the precipitate was washed with THF several times (to remove unbound trioctylamine and unabsorbed PEDOT) and collected by centrifugation; finally the sample was completely dried under vacuum and crushed with a mortar. FT-IR spectra of the solution were recorded on a Bruker EQUINOX55 infrared spectrophotometer by placing drops of pure EDOT or the colloidal solution on CaF_2 crystal slices. Cyclic voltammograms (CVs) were measured with a Zahner IM6e electrochemical workstation, using a glassy carbon electrode (2.25 mm^2) as the working electrode, a Pt wire as the counter electrode, and a saturated calomel electrode (SCE) as the reference electrode. The electrolyte solutions were degassed with nitrogen for 15 min before measurement.

3. Results and Discussion

3.1. Preparation of Gold Nanoparticles with Trioctylamine as the Stabilizer: Spherical Aggregates of Gold Nanoparticles. *3.1.1. Formation of Gold Nanoparticles.* Au colloids were obtained through the reduction of $HAuCl_4$ by EDOT in THF solution at 120 °C with concurrent formation of PEDOT, as supported by UV−vis measurements shown in Figure 1. Figure 1 portrays the characteristic UV−vis absorption spectra of the Au colloid prepared with method I. Before refluxing, the absorption spectrum of the reaction mixture containing 1.9 mM $HAuCl_4$, 4.76 mM EDOT, and 4.76 mM trioctylamine shows a peak at 325 nm (see curve a), which is due to the ligand-to-metal charge-transfer of the $[AuCl_4]^-$ ions.[19] After the solution had been refluxed at 120 °C for 8 h and cooled to room temperature, the peak at 325 nm almost disappeared and the plasmon absorption band of Au nanoparticles at 535 nm appeared (see curve b), indicating that $[AuCl_4]^-$ was reduced by EDOT to produce gold nanoparticles. At the same time, a broad and well-defined absorption band at 744 nm was observed, which could be ascribed to the aggregative states of gold nanoparticles.[20] Aggregation causes the coupling of the plasma modes of the gold nanoparticles, which results in a red shift of the surface plasma resonance in the optical spectrum according

SCHEME 1: Reaction Route of the Preparation of the Gold Colloidal Solution

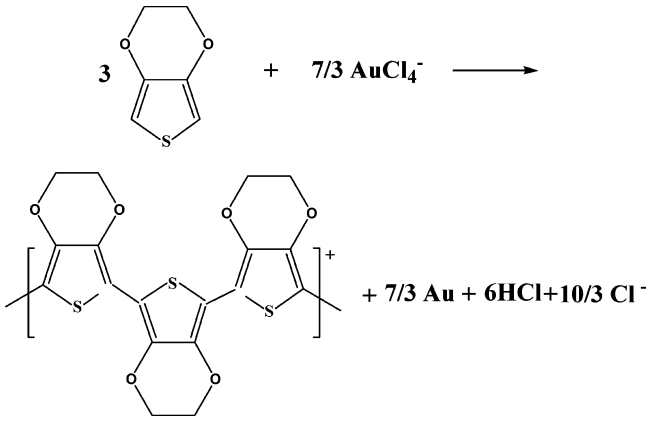

to Mie scattering theory, which is often employed in explaining such red shifts.[21] The theory predicts that shifts in the surface plasma resonance can occur when the particles deviate from spherical geometry, such as occurs in aggregates. In this circumstance the transverse and longitudinal dipole polarizability no longer produce equivalent resonances. Consequently, two plasma resonances appear: a broadened and red-shifted longitudinal plasma resonance and a transverse plasma resonance whose absorbance remains centered at about 540 nm. In addition, the spectrum also exhibits a bipolaron band at about 826 nm and a polaron band at 420 nm stemming from the oxidized PEDOT,[22] which is a byproduct from the oxidation polymerization of EDOT in the process of preparing gold nanoparticles. The chemical conversion is depicted in Scheme 1.

3.1.2. Characterization of the Spherical Aggregates. The Au colloid prepared by method I was characterized by transmission electron microscopy (TEM). Figure 2a shows the representative TEM image. Uniform spherical aggregates with a diameter of about 230 ± 23 nm were observed. The enlarged view (the inset of Figure 2a) clearly shows the edge of a randomly selected spherical aggregate, which consists of individual particles with a size of about 11 nm. The stability of the colloidal solution at room temperature is very good. After 3 months, the TEM image is the same as that of Figure 2a. But the stability at higher temperature is relatively poor; conglomeration takes place to some extent when the temperature is beyond 120 °C. Here, it should be mentioned that the interaction between individual particles is relatively weak and the spherical aggregates could be destroyed by ultrasonic treatment. The spherical aggregates disappeared and individual nanoparticles were monodispersed after ultrasonic treatment (15 min at 40 kHz), as shown in Figure 2b. The results indicate that the spherical aggregates might be formed through intermolecular interaction between nanoparticles.[13]

Figure 3 shows the UV−vis absorption spectra of the spherical aggregates before and after ultrasonic treatment. The plasmon absorption band of the gold nanoparticles at 535 nm remained, but the absorption of the spherical aggregates at 744 nm disappeared after ultrasonic treatment. The results also indicate that the spherical aggregates were composed of individual nanoparticles. As for PEDOT, blue shifts of the bipolaron absorption band from 826 to 780 nm and that of the polaron band from 420 to 383 nm occurred. This variation could be due to the damage of antiparallel dipole interaction between the conjugated backbones of PEDOT molecules in adjacent nanoparticles, which was also reported by Jiang et al.[13] That is to say that an indirect dipole−dipole interaction between the capped PEDOT of adjacent gold nanoparticles was destroyed. Thus, $\pi-\pi$ interaction between the PEDOT-capped nanoparticles could be the driving force for the aggregation of the Au nanoparticles.

In order to confirm the formation of a crystal phase and calculate the mean size of the nanoparticles, X-ray diffraction (XRD) analysis was performed. Figure 4 shows the XRD pattern of the nanoparticles obtained by method I. The diffraction features appearing at $2\theta = 38.20°$, 44.41°, 64.54°, 77.50°, and 81.68° correspond to the (111), (200), (220), (311), and (222) planes of the standard cubic phase of Au, respectively. As expected, the XRD peaks of the nanocrystallites were considerably broadened compared to those of the bulk Au because of the finite size of these crystallites. The average size of the Au particles calculated from the width of the diffraction peak according to the Debye−Scherrer equation[23] is 10.8 nm, which

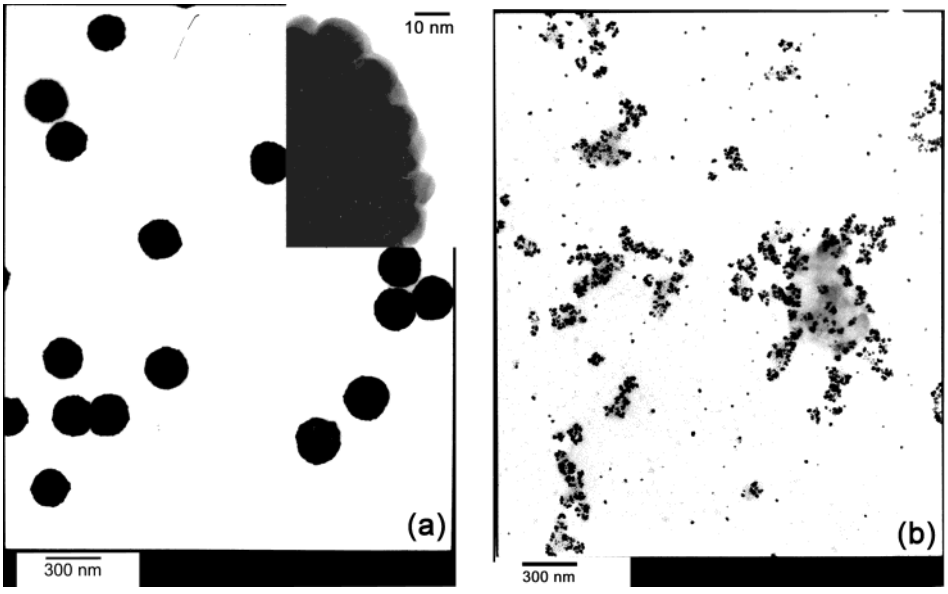

Figure 2. Representative TEM images of (a) the self-assembled microspheres prepared by method I after refluxing for 8 h (the inset shows the enlarged view of the edge of a selected spherical aggregate) and (b) Au nanoparticles after ultrasonic treatment of the Au colloidal solution (at a working frequency of 40 kHz for 15 min).

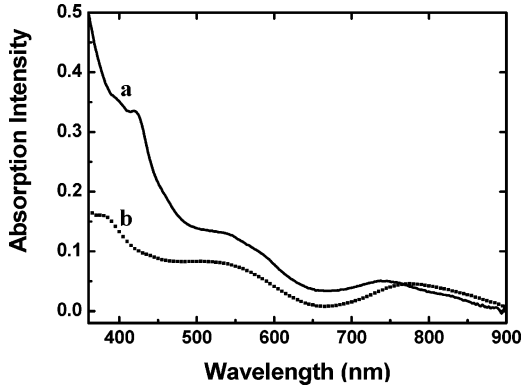

Figure 3. UV−vis absorption spectra of the Au colloidal solution: (a) before and (b) after ultrasonic treatment (at a working frequency of 40 kHz for 15 min).

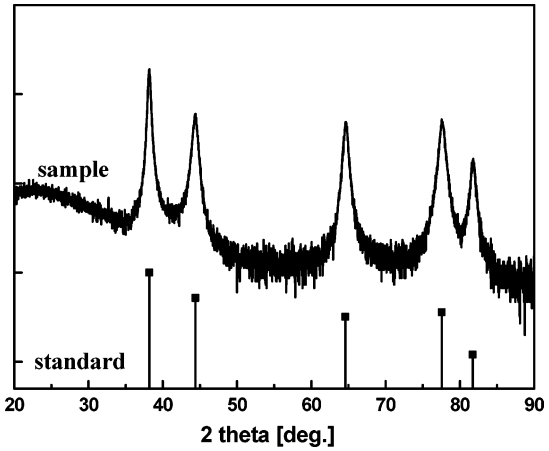

Figure 4. X-ray diffraction pattern of the aggregates of the Au nanoparticles prepared by method I. The vertical lines at the bottom are the reference data for the standard Au crystal taken from powder diffraction file 19-0629 in the database of the International Center for Diffraction Data (ICDD).

is in agreement with the mean size determined by the TEM measurements.

X-ray photoelectron spectroscopy (XPS) was employed to characterize the composition of the gold nanoparticles. The XPS results from the nanoparticles prepared by method I are shown in Figure 5. Figure 5a shows a binding energy of 83.3 eV for Au 4f, which is similar to that of pure Au.[24] The binding energies of 163.4 eV for S and 532.7 eV for O could be respectively ascribed to those of thiophene and the C−O−C unit in EDOT,[25] which indicates that no ring opening of EDOT occurred during the preparation process. Moreover, a very weak peak for nitrogen at 399.7 eV was also detected in the XPS spectra as shown in Figure 5b, which can be ascribed to that of the stabilizer trioctylamine.[26]

The appearance of S and O peaks proposes that as-formed PEDOT is possibly coated on the surfaces of Au nanoparticles. This proposal could be confirmed by the EDS measurement on a gold nanoparticle of as-prepared aggregates as shown in Figure 6. Though the N peak was not detected because of its small atomic number,[27] the appearance of S and O peaks shows that the as-formed PEDOT was indeed coated on the surfaces of gold nanoparticles. In addition, this conclusion could also be supported by the red shift of the surface plasmon absorption. In general, the absorption band of gold nanoparticles with a size of 3−20 nm is located at about 520 nm according to theoretical calculation.[28] In this case, the surface plasmon absorption appeared at 535 nm (see Figure 1), which is 15 nm

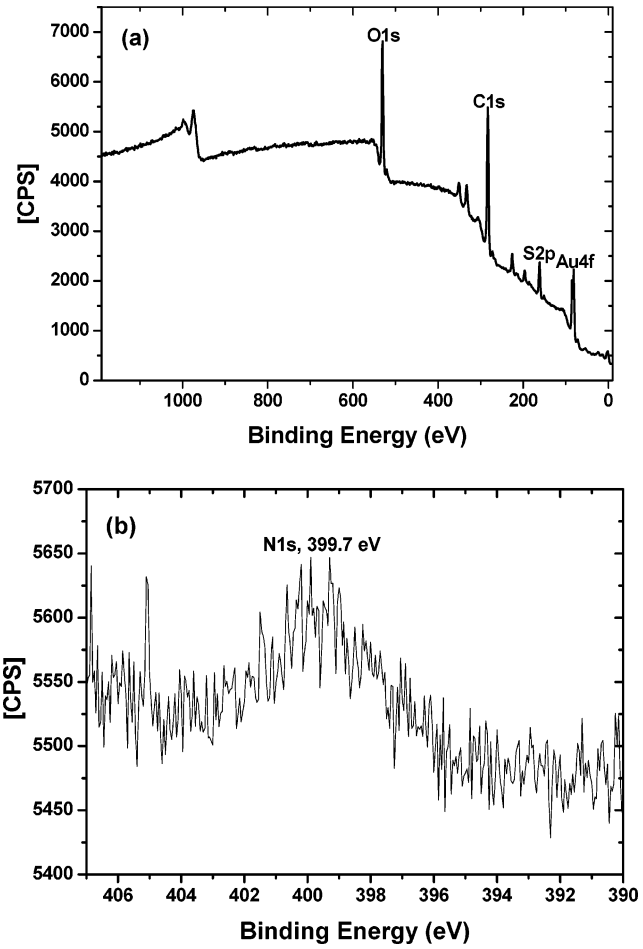

Figure 5. XPS spectra of the Au nanoparticles: (a) XPS survey spectrum of gold; (b) the enlarged spectrum for N1s.

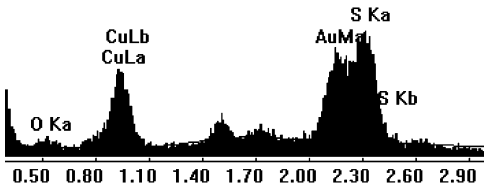

Figure 6. Elemental analysis of a gold nanoparticle in the spherical aggregates by EDS.

red shifted. When the gold nanoparticles were capped with PEDOT, the work function of the gold nanoparticles decreased, which led to the lowering of the energy position of the surface resonance state.[29] As a result, the red shift of the absorption band was produced.[30]

Without trioctylamine as the stabilizer, the solution containing 5 mM EDOT turned green quickly and insoluble precipitates formed after adding the $HAuCl_4$ solution (it should be stated that some precipitates also formed with the lower concentration of trioctylamine). The result shows that only PEDOT could not act as an efficient stabilizer. From the XPS, EDS, and UV−vis spectra results discussed above, the conclusion could be made that the obtained gold nanoparticles were stabilized by trioctylamine and capped with PEDOT.

3.1.3. Formation and Characterization of PEDOT. The UV−vis spectra in Figure 1 indicate the formation of PEDOT (oxidation polymerization of EDOT) along with the production of gold nanoparticles in THF. Here, the formation of PEDOT was further investigated by FT-IR spectroscopy. Figure 7 shows the FT-IR spectra of pure EDOT (see Figure 7a) and that of

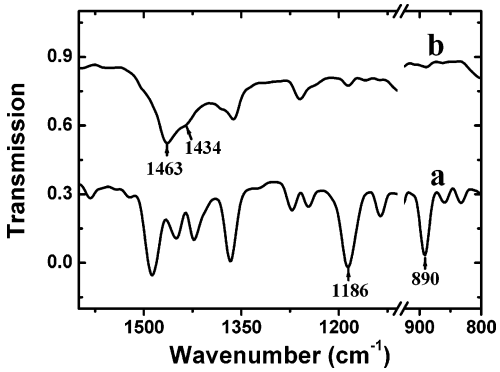

Figure 7. FT-IR spectra of (a) pure EDOT and (b) the Au colloidal solution.

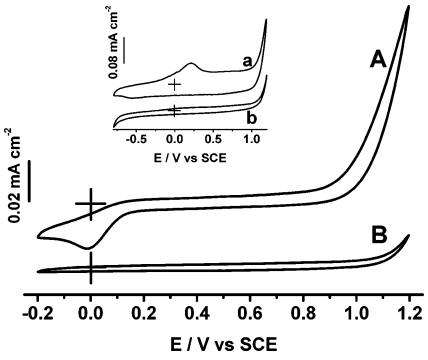

Figure 8. CVs of (A) the 10% (v/v) colloid in 0.1 M $(C_4H_9)_4NPF_6$/THF and (B) blank solution of 0.1 M $(C_4H_9)_4NPF_6$/THF. The scan rate was 10 mV/s. The inset shows the CVs of (a) PEDOT prepared by electrochemical polymerization in 0.1 M $(C_4H_9)_4NPF_6$/THF and (b) blank solution.

the colloidal solution (See Figure 7b). The bands at 1186 and 890 cm^{-1} appeared in the monomer EDOT spectrum, which are attributed to the =C−H in-plane and out-of-plane deformation vibrations, respectively.[25] However, the two bands almost disappeared in the spectrum of the colloidal solution. In addition, the broad band at 1434−1463 cm^{-1} is assigned to the symmetric stretching mode of the aromatic C=C band.[25] The result shows that EDOT was oxidized to form PEDOT by α, α′ coupling.

The electrochemical properties of PEDOT were investigated by cyclic voltammetry as shown in Figure 8. The 10% (v/v) colloidal solution in 0.1M $(C_4H_7)_4NPF_6$/THF shows a reduction peak at −0.02 V (see Figure 8A). The result indicates that the as-formed PEDOT was in the oxidized state, which is consistent with the UV−vis measurement. In addition, the electrochemical response of monomer EDOT was absent in the colloid, which also indicates that all EDOT was oxidized and polymerized to form PEDOT. As a reference, the electrochemical properties of PEDOT prepared by cyclic voltammetry between −0.8 and 1.3 V were also investigated in 0.1M $(C_4H_7)_4NPF_6$/THF as shown in the inset of Figure 8. Compared with the blank solution, an oxidation peak at 0.22 V and a reduction peak at −0.62 V appear. The difference of the reduction peaks between the PEDOT in the Au colloidal solution and the as-prepared PEDOT by the electrochemical method implies that the as-formed PEDOT in the colloidal solution has a shorter conjugation chain. In fact, the formed PEDOT in the colloidal solution is a kind of oligomer of EDOT.

3.1.4. Formation Mechanism of the Spherical Aggregates. On the basis of the discussion above, a model of the formation mechanism for the spherical aggregates is proposed as shown in Scheme 2. The formation of the spherical aggregates is divided into two stages. The first stage is the formation of the

SCHEME 2: Model Proposed for the Self-Assembling Process of Individual Nanoparticles to Form Microspheres through $\pi-\pi$ Interaction

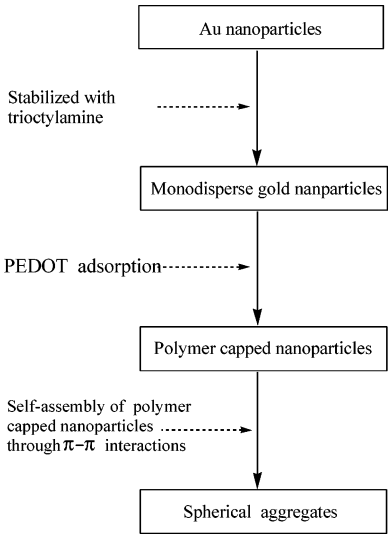

individual trioctylamine-stabilized and PEDOT-capped gold nanoparticles. Monodispersed gold nanoparticles stabilized by trioctylamine are produced with the concurrent formation of the oxidized PEDOT in the beginning of the preparation reaction (which is verified by the sample with a short refluxing time of the reaction solution). Since the amine−Au interaction is relatively weak,[31] these trioctylamine-stabilized Au nanoparticles tend to aggregate. On the other hand, the oxidized PEDOT coated on the Au nanoparticles possesses a delocalized positive charge and provides both steric and electrostatic stabilization, which will enhance the stability of the Au particles colloid.[32] So, it could be considered that the growth of the nanoparticles is controlled by the competition between the stabilizing effect of the trioctylamine and the capping of the oxidized PEDOT. The competition results in the formation of the gold nanoparticles stabilized with trioctylamine and capped by PEDOT. The second stage is the self-assembly of the gold nanoparticles into uniform spherical aggregates through $\pi-\pi$ interaction between the PEDOT capped on the individual nanoparticles. Each Au nanoparticle could gather the neighboring particles within its individual field of attraction, which extends as a circular arc around a spherical particle to a defined distance from the center of the particle according to the theory of diffusion-controlled growth.[13] So, the aggregates tend to be spherical. Meanwhile, the growth of the microspheres is influenced strongly by the variation of their surface energy with size.[33] Thus, the aggregates also tend to grow into a spherical shape in order to minimize the surface energy of the aggregates.

3.2. Preparation of Gold Nanoparticles with Trioctylamine as the Stabilizer: The Effects of Reaction Time and the Concentration of EDOT. The growth process of the uniform spherical aggregates was investigated in order to check the effect of reaction time on the aggregation. Samples at different reaction periods, such as those refluxed for 4 h and 6 h, were examined by TEM. In the case of samples refluxed for 4 h, irregular aggregates with an average size of about 130 nm and dispersed nanoparticles with a size of about 2 nm were observed, as shown in Figure 9a. For the sample refluxed for 6 h (shown in Figure 9b), the irregular aggregates turned into spherical aggregates with a diameter of about 160 nm, and the individual small-sized (ca. 2 nm) gold nanoparticles were still dispersed around the aggregates. In contrast with those samples refluxed for 4 h and 6 h, the sample refluxed for 8 h

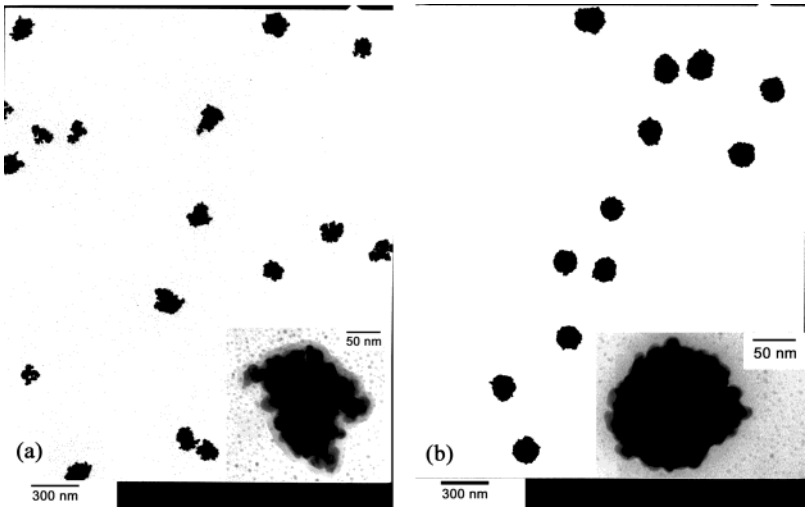

Figure 9. Representative TEM images of (a) aggregates of the gold nanoparticles after refluxing for 4 h (the enlarged view of an aggregate is shown in the inset) and (b) spherical aggregates of the gold nanoparticles after refluxing for 6 h (the inset shows the enlarged image of an aggregate).

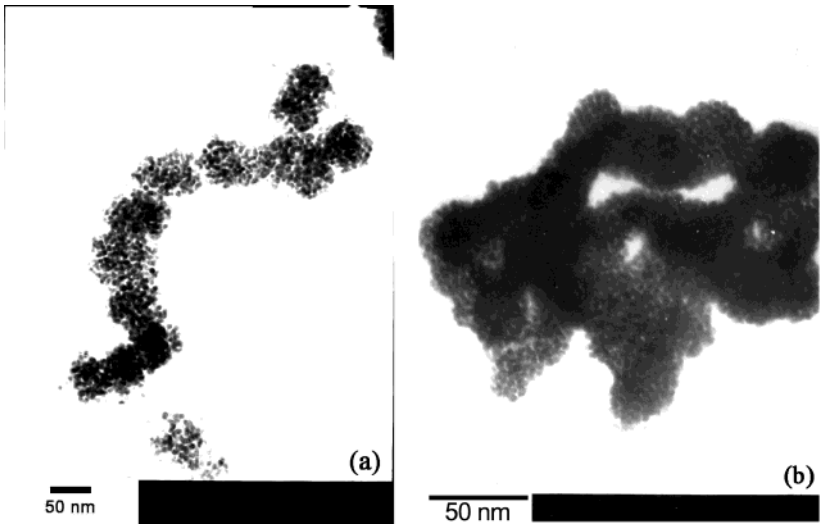

Figure 10. TEM images of (a) loose spherical aggregates of the Au nanoparticles prepared by method II and (b) connected spherical aggregates of the Au nanoparticles prepared by method III.

exhibited only spherical and uniform aggregates of approximately 230 ± 23 nm, and the dispersed small gold nanoparticles were not detected (see Figure 2a). The results agree with the mechanism proposed above; that is, small particles (ca. 2 nm) may be first formed, which then grow into larger ones (ca. 11 nm) which build up the spherical aggregates, and the spherical aggregates then form gradually with the proceeding of the reaction process.

In addition to the influence of the refluxing time on the aggregation of the Au nanoparticles, the concentration of the reductant also affected the aggregation morphology. Figure 10 shows the representative TEM images of the Au nanoparticles obtained with the higher concentration of EDOT used in methods II and III. In comparison with method I, the concentration of EDOT in method II was 2 times higher and that in method III was 3 times higher. In the case of method II, the TEM image (Figure 10a) clearly illustrates the existence of a number of spherical aggregates with a smaller size of about 50 nm, which further aggregate into a wirelike configuration. For the sample obtained by method III, the TEM image (Figure 10b) displays the interconnected spherical aggregates with a size of about 60−80 nm. The mean size of the Au nanoparticles, which self-assembled into the spherical aggregates, was 7.2 nm for sample II (obtained by method II) and 5.8 nm for sample III. Obviously, the mean size of the Au nanoparticles decreased with the increase of the concentration of EDOT. From the viewpoint of the particle nucleation and growth, a fast reduction rate of Au (III) caused by increasing the EDOT concentration could lead to the generation of smaller Au nanoparticles because of the nucleation process predominating over the growth process. In addition, the excess amount of EDOT in the solution may affect the aggregation of the Au nanoparticles, which results in the loose spherical aggregates obtained with method II and the interconnected aggregates formed with method III.

3.3. Preparation of Gold Nanoparticles with Trioctylamine as the Stabilizer: Hollow Spheres Composed of Gold Nanoparticles. The representative TEM images of the sample prepared by method IV exhibit hollow spheres as shown in Figure 11. Enlarged hollow spheres with a shell thickness of 10−30 nm are shown in parts b and c of Figure 11. The hollow spheres are composed of small gold nanoparticles with an average size of 1.8 nm. The stability of the hollow spheres at room temperature is also very good. After 3 months, the TEM image remains unchanged.

In method IV, the concentration of the reductant EDOT is the same as that in method III (which is 3 times higher than

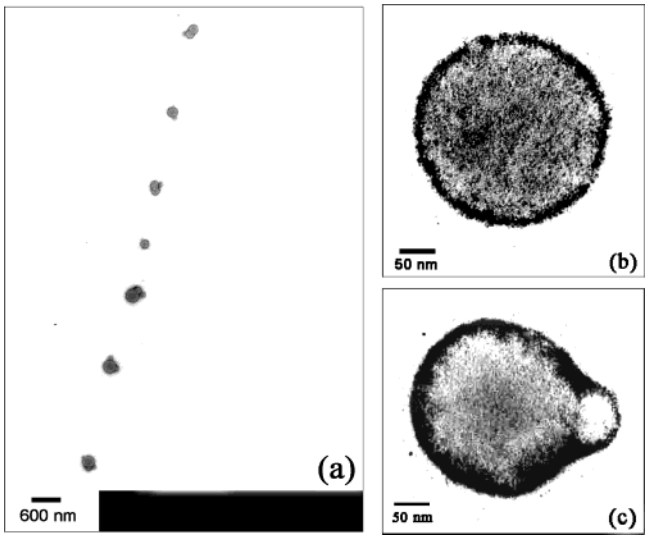

Figure 11. Representative TEM images of (a) spherical hollow aggregates of the Au nanoparticles prepared by method IV and (b−c) the enlarged views of the hollow spheres aggregates.

that in method I), and the concentration of the stabilizer trioctylamine is 3 times higher than those in methods I−III. According to the formation mechanism for the gold nanoparticles discussed above, the higher concentration of EDOT will lead to the formation of smaller-sized gold nanoparticles. Moreover, the higher concentration of trioctylamine could efficiently limit the growth of the Au nanoparticles further due to its stabilizing effect on the nanoparticles. As a result, the smallest gold nanoparticles with a size of 1.8 nm were obtained with method IV.

The formation mechanism of the hollow sphere, which might be related to the excess amount of trioctylamine in the solution, could be different from that of the spherical aggregates. The excess trioctylamine may retard the formation of the spherical aggregates in the colloidal solution. The formation process of the hollow spheres might be induced by solvent evaporation. When we prepare the sample for the TEM measurement, a drop of the Au colloidal solution is placed on a copper grid and dried slowly at room temperature. The colloidal solution contains the solvents THF and a little water. In the evaporation process, preferential evaporation of the more volatile THF over water could lead to a phase separation between water and the trioctylamine-stabilized Au colloidal solution. Because of the amphiphilic nature of trioctylamine, it could be speculated that the gold nanoparticles stabilized by excessive trioctylamine would gather around the residual water: the hydrophobic long-tailed alkyl groups in trioctylamine spread outward and the hydrophilic groups connected with the gold nanoparticles spread toward the inner water. Thus, the evaporation process leads to the formation of micelle-like "core−shell" structures, with water acting as the "core" and the gold nanoparticles stabilized by trioctylamine acting as the "shell". The flexible water "core" could deviate from a standard sphere, or the "core/shell" structures could coalesce to form intersectional structures in the process of the subsequent evaporation of the water. After the evaporation of the water is finished, hollow nanoshells composed of the gold nanoparticles will be formed as those in parts b and c of Figure 11. Through a similar solvent evaporation method, Bruinsma et al.[34] synthesized hollow spherical mesoporous silica. Thus, this simple approach could be extended to prepare hollow nanoshells composed of other inorganic materials.

3.4. Preparation of Gold Nanoparticles with Dioctylamine as the Stabilizer. To further investigate the effect of the stabilizer on the morphology of the Au nanoparticles, we also used other alkylamines instead of trioctylamine as the stabilizer in the preparation of the Au colliodal solutions. The alkylamines used include dioctylamine, octylamine, dodecylamine, and octodecylamine. Au nanoparticles with a narrow size distribution were produced with these stabilizers, but the aggregation behavior of the Au nanoparticles was different from that produced with trioctylamine as the stabilizer. Here, detailed results are presented only for the samples with dioctylamine as the stabilizer in order to avoid verbosity of the text.

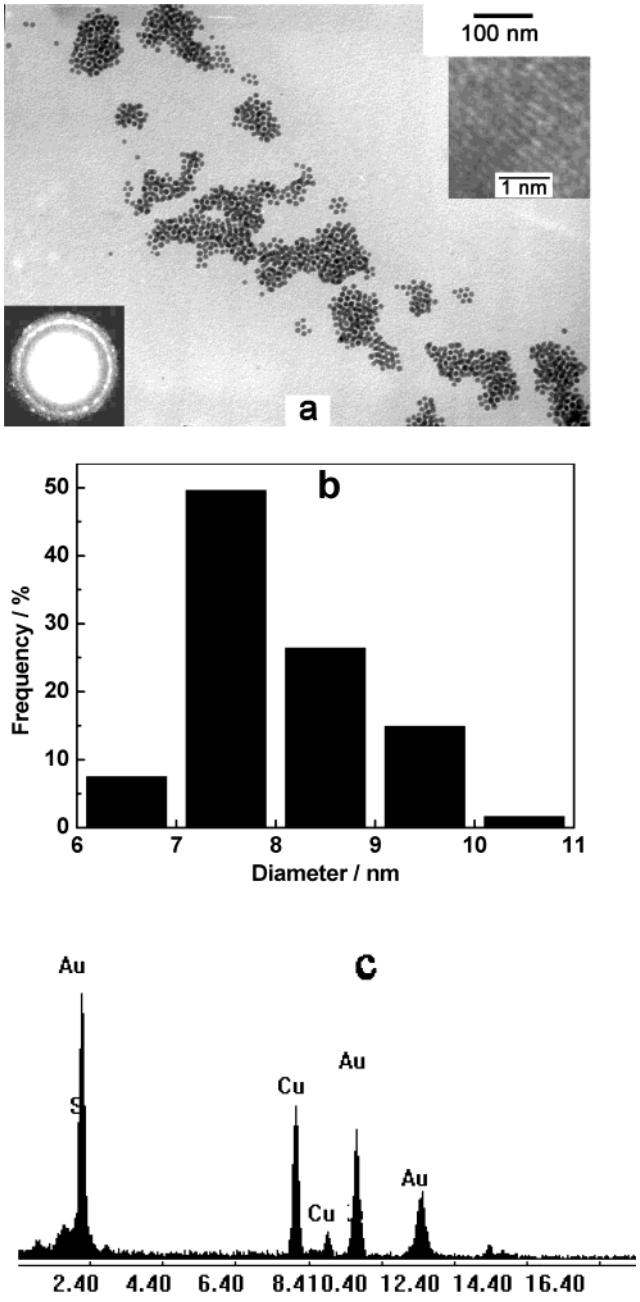

Figure 12. (a) Representative TEM image of the gold nanoparticles synthesized by method V (the insets present the SAED pattern (lower left) and a HRTEM image for a single Au nanoparticle (upper right)); (b) the size distribution histogram of the Au nanoparticles; (c) elemental analysis of a single Au nanoparticle by EDS.

The Au colloid prepared by method V, where dioctylamine was used as the stabilizer, was examined by TEM. The representative TEM image and the corresponding size distribution histogram of the as-prepared Au nanoparticles are shown in parts a and b of Figure 12, respectively. It can be seen that

uniform nanoparticles were obtained with dioctylamine as the stabilizer (see Figure 12a). There is no spherical aggregation of the nanoparticles observed with trioctylamine as the stabilizer. Instead, the nanoparticles self-assembled into close-packed arrays. The dark ring patches also indicate the existence of a bilayer structure of the particles. The same pattern was also reported by Schiffrin et al.[35] The nanocrystals in the top layer occupy 2-fold saddle sites to form hexagonal rings, which are rotated by 30° relative to the lower layer. Figure 12a also shows the SAED pattern (lower left inset) and the HRTEM image (upper right inset) of a randomly selected nanoparticle. The SAED pattern shows the crystalline feature of the Au nanoparticles. And from the HRTEM image, we could notice that these crystalline Au nanoparticles have faceted structures and the distance between the lattice planes is $d_{111} = 2.4$ Å. The histogram in Figure 12b illustrates that the mean size of the Au nanoparticles is 8.03 nm with a standard deviation of 0.89 nm.

Energy-dispersive X-ray spectroscopy (EDS) was also employed to determine the chemical composition of the gold nanoparticles, as shown in Figure 12c. The EDS spectrum obtained from a randomly selected nanoparticle shows the peaks for Au and S together with the peaks for Cu. The Cu peaks are due to the copper grid used in the sample preparation. The appearance of the S peak indicates that the as-prepared Au nanoparticles are capped with PEDOT, but the N peak corresponding to dioctylamine was not detected because of its low content and small atomic number.[27]

4. Conclusions

In this work, a novel reductant, EDOT, was first used for preparing gold nanoparticles in THF solution with the concurrent formation of PEDOT. With trioctylamine as the stabilizer, the gold nanoparticles produced were stabilized by trioctylamine and capped by PEDOT. The nanoparticles could self-assemble into spherical aggregates by $\pi-\pi$ interaction between PEDOT capped on the individual particles. The size of the Au nanoparticles and the morphology of the aggregates can be regulated by changing the reaction time and the concentrations of EDOT and trioctylamine. Higher concentration of EDOT resulted in smaller Au particle sizes and loose aggregation. At an appropriate concentration of the reactive agents and reaction time, uniform spherical aggregates of Au nanoparticles were observed. Meanwhile, the formed PEDOT is a kind of oligomer with a relatively shorter conjugation chain. Hollow spherical aggregates of the Au nanoparticles were observed with a higher concentration of trioctylamine and a higher concentration of EDOT in the preparation solution. With dioctylamine as the stabilizer, homogeneous gold nanoparticles were obtained, and the nanoparticles could self-assemble into an ordered structure.

Acknowledgment. This work was supported by the State Key Basic Research Project of the Ministry of Science and Technology of China (No. 2001CB610507).

References and Notes

(1) Schmid, G. *Chem. Rev.* **1992**, *92*, 1709.
(2) Cosandey, F.; Madey, T. E. *Surf. Rev. Lett.* **2001**, *8*, 73.
(3) Bamwenda, G. R.; Tsubota, S.; Nakamura, T.; Haruta, M. *Catal. Lett.* **1997**, *44*, 83.
(4) Valden, M.; Lai, X.; Goodman, D. W. *Science.* **1998**, *281*, 1647.
(5) Brown, L.; Hutchison, J. *J. Phys. Chem. B* **2001**, *105*, 8911.
(6) Whetten, R.; Khoury, J.; Alvarez, M.; Murthy, S.; Vezmar, I.; Wang, Z.; Stephens, P.; Cleveland, C.; Luedtke, W.; Landman, U. *Adv. Mater.* **1996**, *8*, 428.
(7) Turkevich, J.; Stevenson, P. C.; Hiller, J. *Discuss. Faraday Soc.* **1951**, *11*, 55.
(8) Enustun, B.; Turkevich, J. *J. Am. Chem. Soc.* **1963**, *85*, 3317.
(9) Brust, M.; Walker, M.; Bethell, D.; Schiffrin, D. J.; Whyman, R. *J. Chem. Soc., Chem. Commun.* **1994**, *7*, 801.
(10) Sarathy, K. V.; Raina, G.; Yadav, R. T.; Kulkarni, G. U.; Rao, C. N. R. *J. Phys. Chem. B* **1997**, *101*, 9876.
(11) Dai, X.; Tan, Y.; Xu, J. *Langmuir* **2002**, *18*, 9010.
(12) Zhou, Q.; Bao, J.; Xu, Z. *J. Mater. Chem.* **2002**, *12*, 384.
(13) Jin, J.; Iyoda, T.; Cao, C.; Song, Y.; Jiang, L.; Li, T.; Zhu, D.; *Angew. Chem., Int. Ed.* **2001**, *40*, 2135.
(14) Youk, J.; Locklin, J.; Xia, C.; Park, M.; Advincula, R. *Langmuir* **2001**, *17*, 4681.
(15) Granström, M.; Berggren, M.; Inganäs, O. *Science* **1995**, *267*, 1479.
(16) Heywang, G.; Joans, F. *Adv. Mater.* **1992**, *4*, 116.
(17) Bayer, A. G. U.S. Patent 5, 035, 926, **1991**.
(18) De Leeuw, D. M.; Kraakman, R. A.; Bongaerts, P. F. G.; Mutsaers, C. M. J.; Klaasen, D. B. M. *Synth. Met.* **1994**, *66*, 263.
(19) Thomas, K. G.; Zajicek, J.; Kamat, P. V. *Langmuir* **2002**, *18*, 3722.
(20) Shipway, A. N.; Lahav, M.; Gabai, R.; Willner, I. *Langmuir* **2000**, *16*, 8789.
(21) (a) Mie, G. *Ann. Physik* **1908**, *25*, 377. (b) Kreibig, U.; Genzel, L. *Surf. Sci.* **1985**, *156*, 678. (c) Creighton, J. A.; Eadon, D. G. J. Chem. Soc., *Faraday Trans.* **1991**, *87*, 3881. (d) Norman, T. J., Jr.; Grant, C. D.; Magana, D.; Zhang, J.; Liu, J.; Cao, D.; Bridges, F.; Van Buuren, A. *J. Phys. Chem. B* **2002**, *106*, 7005.
(22) Pei, Q.; Zuccarello, G.; Ahlskog, M.; Inganäs, O. *Polymer* **1994**, *35*, 1347.
(23) Cullity, B. D. *Elements of X-ray Diffraction*, 2nd ed.; Addision-Wesley: Menlo Park, CA, 1978.
(24) Hüfner, S. *Photoelectron Spectroscopy*, 2nd ed.; Springer-Verlag: New York, 1996.
(25) Sakmeche, N.; Aeiyach, S.; Aaron, J.; Jouini, M.; Lacroix, J. C.; Lacaze, P. *Langmuir* **1999**, *15*, 2566.
(26) Leff, D. V.; Brandt, L.; Heath, J. R. *Langmuir* **1996**, *12*, 4723.
(27) Tan, Y. W.; Jiang, L.; Li, Y. F.; Zhu, D. B. *J. Phys. Chem. B* **2002**, *106*, 3131.
(28) Dalmia, A.; Lineken, C. L.; Savinell, R. F. *J. Colliod Interface Sci.* **1998**, *205*, 535.
(29) Wolf, M.; Knoesel, E.; Hertel, T. *Phys. Rev. B* **1996**, *54*, R5295.
(30) Sandhyarani, N.; Pradeep, T. *J. Mater. Chem.* **2000**, *10*, 981.
(31) Heath, J. R.; Knobler, C. M.; Leff, D. V. *J. Phys. Chem.* **1997**, *101*, 189.
(32) Zhou, Y.; Itoh, H.; Uemura, T.; Naka, K.; Chujo, Y. *Langmuir* **2002**, *18*, 277.
(33) Peng, X. G.; Wickham, J.; Alivisatos, A. P. *J. Am. Chem. Soc.* **1998**, *120*, 5343.
(34) Bruinsma, P. J.; Kim, A. Y.; Liu, J.; Baskaran, S. *Chem. Mater.* **1997**, *9*, 2507.
(35) Fink, J.; Kiely, C. J.; Bethell, D.; Schiffrin, D. J. *Chem. Mater.* **1998**, *10*, 922.